Am J Physiol Renal Physiol 305: F545–F552, 2013.
First published May 15, 2013; doi:10.1152/ajprenal.00234.2013.

Functioning of an arteriovenous fistula requires heme oxygenase-2

Lu Kang,[1] Joseph P. Grande,[2] Gianrico Farrugia,[3] Anthony J. Croatt,[1] Zvonimir S. Katusic,[4] and Karl A. Nath[1]

[1]*Division of Nephrology and Hypertension, Department of Medicine, Mayo Clinic, Rochester, Minnesota;* [2]*Department of Laboratory Medicine and Pathology, Mayo Clinic, Rochester, Minnesota;* [3]*Division of Gastroenterology and Hepatology, Department of Medicine, Mayo Clinic, Rochester, Minnesota; and* [4]*Departments of Anesthesiology and Molecular Pharmacology and Experimental Therapeutics, Mayo Clinic, Rochester, Minnesota*

Submitted 25 April 2013; accepted in final form 10 May 2013

Kang L, Grande JP, Farrugia G, Croatt AJ, Katusic ZS, Nath KA. Functioning of an arteriovenous fistula requires heme oxygenase-2. *Am J Physiol Renal Physiol* 305: F545–F552, 2013. First published May 15, 2013; doi:10.1152/ajprenal.00234.2013.—Heme oxygenase-2 (HO-2), the constitutive isoform of the heme-degrading enzyme heme oxygenase, may serve as an anti-inflammatory vasorelaxant, in part, by generating carbon monoxide. Arteriovenous fistulas (AVFs) are employed as hemodialysis vascular accesses because they provide an accessible, high-blood-flow vascular segment. We examined the role of vascular expression of HO-2 in AVF function. An AVF was created in mice by anastomosing the carotid artery to the jugular vein. HO-2 expression was detected by immunohistochemistry in the intact carotid artery, mainly in endothelial cells and smooth muscle cells; expression of HO-2 protein and mRNA was modestly increased in the artery of the AVF. Creating an AVF in HO-2$^{-/-}$ mice compared with an AVF in HO-2$^{+/+}$ mice led to markedly reduced AVF blood flow and increased numbers of nonfunctioning AVFs. The impairment of AVF function in the setting of HO-2 deficiency could not be ascribed to either preexisting intrinsic abnormalities in endothelium-dependent and endothelium-independent relaxation of the carotid artery in HO-2-deficient mice or to impaired vasorelaxant responses in the intact carotid artery in vivo. HO-1 mRNA was comparably induced in the AVF in HO-2$^{+/+}$ and HO-2$^{-/-}$ mice, whereas the AVF in HO-2$^{-/-}$ mice compared with that in HO-2$^{+/+}$ mice exhibited exaggerated induction of matrix metalloproteinase (MMP)-9 but similar induction of MMP-2. HO-2 deficiency also led to lower AVF blood flow when AVFs were created in uremia, the latter induced by subtotal nephrectomy. We conclude that HO-2 critically contributes to the adequacy of AVF blood flow and function.

arteriovenous fistula; heme oxygenase-2; hemodialysis; vascular access

HEME OXYGENASE (HO) represents the major mechanism whereby heme is degraded, and such activity exists in two isoforms, the inducible, HO-1, and the constitutive, HO-2. In addition to degrading heme, either HO isoform generates carbon monoxide, bile pigments, and iron, the latter sequestered by ferritin or exported extracellularly by ferrportin (1, 31). Carbon monoxide, among its other properties, is recognized as a vasorelaxant molecule as well as an anti-inflammatory one, and bile pigments can exert antioxidant and anti-inflammatory effects. Through these and other actions, HO-1 has been shown to be a protectant in diverse models of tissue injury. Interest also exists regarding the protective effects of HO-2 in tissue injury, but thus far this area has received substantially less attention compared with the study of HO-1 (1, 31).

We previously demonstrated that induction of HO-1 is a beneficial response following the creation of an arteriovenous fistula (AVF) (20), a study motivated by the recognition of the pressing problem of hemodialysis vascular access dysfunction and the need for new therapeutic strategies for such dysfunction (2, 16, 22, 26, 27, 40, 41, 45). As emphasized by the Fistula First Initiative, the AVF is the preferred hemodialysis vascular access because such accesses, compared with arteriovenous grafts and central venous hemodialysis catheters, exhibit greater duration in function, are attended by less morbidity and mortality, and incur lower costs (2, 16, 22, 26, 27, 40, 41, 45). However, the outcomes for AVFs created for use as hemodialysis vascular accesses are decidedly grim: *1*) ~50% of all such accesses never become sufficiently functional such that they can ever be used as hemodialysis vascular accesses; *2*) mature and usable AVFs often require repeated interventions to maintain functionality; and *3*) the overall longevity of a functional AVF is relatively limited, commonly necessitating the placement of subsequent vascular accesses during the lifetime of the hemodialysis patient. Understanding the mechanisms whereby AVFs either fail to mature or decline in function is thus a critical issue in the care of patients with chronic kidney disease (CKD).

The present study was undertaken to determine whether HO-2 contributes to the functionality of an AVF, hypothesizing that a constitutive isoform of HO, already in place in the vasculature at the time of AVF creation (and distinct from HO-1, which requires induction), would be conducive to the ensuing and expected augmentation of blood flow once an AVF is created. Because AVF function is defined by blood flow through the AVF, this quantitative index comprised our principal approach in assessing AVF function.

Our evaluation of the role of HO-2 involved a multilayered approach that included the following studies: examination of vascular expression of HO-2; the creation of AVFs in HO-2$^{+/+}$ and HO-2$^{-/-}$ mice; the in vitro assessment of vasorelaxant responses of the same artery (carotid) used in the AVF in HO-2$^{+/+}$ and HO-2$^{-/-}$ mice; the in vivo assessment of acute increments in carotid blood flow in response to acetylcholine in HO-2$^{+/+}$ and HO-2$^{-/-}$ mice; and examination of the role of HO-2 in augmenting AVF blood flow in uremia, the latter induced by subtotal nephrectomy before the creation of the AVF.

MATERIAL AND METHODS

Murine AVF model. All studies were approved by the Institutional Animal Care and Use Committee of Mayo Clinic and performed

Address for reprint requests and other correspondence: K. A. Nath, Mayo Clinic, Guggenheim 542, 200 First St. SW, Rochester, MN 55905 (e-mail: nath.karl@mayo.edu).

1931-857X/13 Copyright © 2013 the American Physiological Society

Downloaded from journals.physiology.org/journal/ajprenal (065.021.193.086) on March 2, 2022.

according to the guidelines of the National Institutes of Health. In these studies, a murine AVF model created by an end-to-side anastomosis between the right carotid artery and jugular vein was employed, as we described previously (19, 20, 21). In initial studies, male C57Bl6J mice (Jackson Laboratory, Bar Harbor, ME) ranging from 9–12 wk of age were employed to characterize HO-2 expression in the arterial limb of the murine AVF. To determine the functional significance of HO-2 in the AVF, we utilized HO-$2^{+/+}$ and HO-$2^{-/-}$ mice, which we have employed in prior studies (13, 32). Colonies of these mice having targeted disruption of the HO-2 gene, as described by Poss and Tonegawa (37), were maintained by mating of HO-$2^{+/-}$ males and females and were genotyped at the time of weaning using a PCR method. Mice were age matched (in the range of 18–35 wk) and sex matched for these studies. AVFs were created in HO-$2^{+/+}$ and HO-$2^{-/-}$ mice, and the nonoperated, contralateral carotid arteries were used as controls. Four weeks after the creation of the AVF, blood flow through the AVF and the contralateral carotid artery was measured using a perivascular flow meter (TS420; Transonic Systems), as we previously described (21). In addition, assessment of gene expression was performed on the arterial limb of the AVF and the contralateral carotid artery of HO-$2^{+/+}$ and HO-$2^{-/-}$ mice 1 wk after the creation of the AVF.

Murine model of CKD. For studies examining the effect of HO-2 deficiency on AVF blood flow in uremia, CKD was induced in mice by subtotal nephrectomy, the latter based on a two-step renal ablation procedure as described by Gagnon and Duguid (14, 15). Briefly, in the first step, mice were anesthetized with pentobarbital sodium (60 mg/kg ip) and, via a 2-cm flank incision, the upper third and lower third of the right kidney were ablated by electrocautery. In the second surgery, the left kidney was removed 1 wk later. Control animals received sham operations that included flank incisions and exposure of kidneys. Seven to 10 days after the second surgery, renal function was assessed by measurement of blood urea nitrogen (BUN) levels (Urea Nitrogen Assay kit; Pointe Scientific, Canton, MI). As described previously (14, 15), this CKD model resulted in an approximate doubling of BUN levels, which did not progress over the time course of these studies. At 2 wk after the second surgery, an AVF was created as described above.

Measurement of increments in carotid artery blood flow induced by acetylcholine in vivo. Blood flow responses to acetylcholine were determined in the carotid arteries of HO-$2^{+/+}$ and HO-$2^{-/-}$ mice, as described previously (21). Briefly, following baseline flow measurements, the carotid artery was bathed in a solution of acetylcholine (100 μM in normal saline; Sigma, St. Louis, MO), and the solution was refreshed every 2 min for the duration of the study. Ten minutes after acetylcholine treatment commenced, blood flow was again determined.

Assessment of mRNA expression by quantitative real-time RT-PCR. Gene expression in carotid arteries was assessed by quantitative real-time RT-PCR, as previously described (19, 20, 36). Total RNA was extracted and further purified using the TRIzol method (Invitrogen, Carlsbad, CA) and an RNeasy Mini kit (Qiagen, Valencia, CA), respectively, and cDNA was synthesized employing random hexamers (Transcriptor First-Strand cDNA Synthesis kit; Roche Applied Science, Indianapolis, IN). The probe and primers used for these assessments were obtained as assay sets (TaqMan Gene Expression Assays; Applied Biosystems, Foster City, CA) and employed with the following parameters: 10 min at 95°C, followed by 40 cycles of amplification for 15 s at 95°C and 1 min at 60°C. Expression of 18S rRNA was similarly determined and used for normalization of target mRNA expression.

Assessment of vascular reactivity in carotid arteries. Vascular reactivity was examined in mouse carotid arteries as described in our prior studies (11, 12). Briefly, carotid arteries were carefully removed and placed immediately into cold (4°C) modified Krebs-Ringer bicarbonate solution containing (in mM) 118.6 NaCl, 4.7 KCl, 2.5 $CaCl_2$, 1.2 $MgSO_4$, 1.2 KH_2PO_4, 25.1 $NaHCO_3$, 0.026 EDTA, and 10.1 glucose. After careful dissection to remove connective tissue, segments (4 mm long) of carotid arteries were transferred to small vessel chambers (Living Systems Instrumentation, St. Albans, VT) filled with Krebs-Ringer bicarbonate solution with continuous aeration (94% O_2 and 6% CO_2 gas) at 37°C. Proximal and distal ends of the vessels were mounted and sutured onto two small glass microcannulas (positioned in the vessel chamber). The transluminal pressure of 50 mmHg was set at a level that was found to be optimal for contractions to U-46619 (3×10^{-8} M). Endothelium-dependent relaxations to acetylcholine (10^{-9} to 10^{-5} M) were first obtained after stabilization of submaximal contraction to the thromboxane analog U-46619 (3×10^{-8} to 10^{-7} M). Concentration-dependent responses to diethylammonium(*Z*)-1-(*N*,*N*-diethylamino)diazen-1-ium-1,2-diolate (DEA NONOate; 10^{-9} to 10^{-5} M) were obtained in carotid arteries after submaximal contraction to U-46619 (3×10^{-8} to 10^{-7} M). Relaxation responses were then calculated as a percentage of maximal relaxation induced by 3×10^{-4} M papaverine.

Immunohistochemical localization of HO-2 expression. Immunohistochemical analysis of HO-2 expression was performed, as described previously, on 5-μm sections prepared from formalin-fixed, paraffin-embedded arterial limbs of the AVF and in contralateral control carotid arteries. A rabbit polyclonal antibody (catalog no. ADI-SPA-897) was used as the primary antibody (20, 44).

Histological evaluation of the AVF. A semiquantitative analysis of luminal narrowing in the juxta-anastomotic regions of the AVF in HO-$2^{+/+}$ and HO-$2^{-/-}$ mice was performed (44). Hematoxylin- and eosin-stained sections were assessed for the degree of neointimal hyperplasia, mural thrombus formation, and vessel wall thickening, and the percentage of AVFs exhibiting luminal narrowing >50% and 75% were determined.

Statistical analysis. Results are means ± SE and considered statistically significant for $P < 0.05$. The Student's *t*-test was used for parametric data, and the Mann-Whitney *U*-test was employed for nonparametric data. AVF failure was assessed using Fisher's exact test.

RESULTS

Immunohistochemical studies of the intact carotid artery demonstrated that HO-2 was expressed in the endothelium and smooth muscle cell layer under basal conditions and that such cellular expression appeared more prominent in the AVF in wild-type C57Bl6 mice 2 wk after AVF creation (Fig. 1). At earlier time points, HO-2 mRNA expression in the AVF was unchanged at 3 days and modestly increased at 7 days following the creation of the AVF (Fig. 2). This mRNA temporal profile for HO-2 significantly contrasted with that displayed by HO-1 mRNA; in the same arterial segments of the AVF at these same time points, HO-1 mRNA was markedly induced (10- and 7-fold, respectively) in the AVF (Fig. 3).

To determine the functional significance of HO-2 in the AVF, the AVF was created in HO-$2^{+/+}$ and HO-$2^{-/-}$ mice. HO-$2^{+/+}$ and HO-$2^{-/-}$ mice derived from a colony originally generated by Poss and Tonegawa (37) and maintained by our laboratories (13, 32) have comparable growth, body weights, and systolic blood pressure. For example, in cohorts of HO-$2^{+/+}$ and HO-$2^{-/-}$ mice with matched numbers of male and female mice and of comparable age (29 ± 1 and 28 ± 1 wk), the body weights (31 ± 2 and 30 ± 1 g) and systolic blood pressures (114 ± 3 and 110 ± 4 mmHg) were not significantly different.

Creation of the AVF, as expected, led to increased carotid blood flow in the AVF compared with that in the contralateral intact carotid artery in HO-$2^{+/+}$ mice and as measured at 4 wk after the creation of the AVF (Fig. 4). Remarkably, this

Downloaded from journals.physiology.org/journal/ajprenal (065.021.193.086) on March 2, 2022.

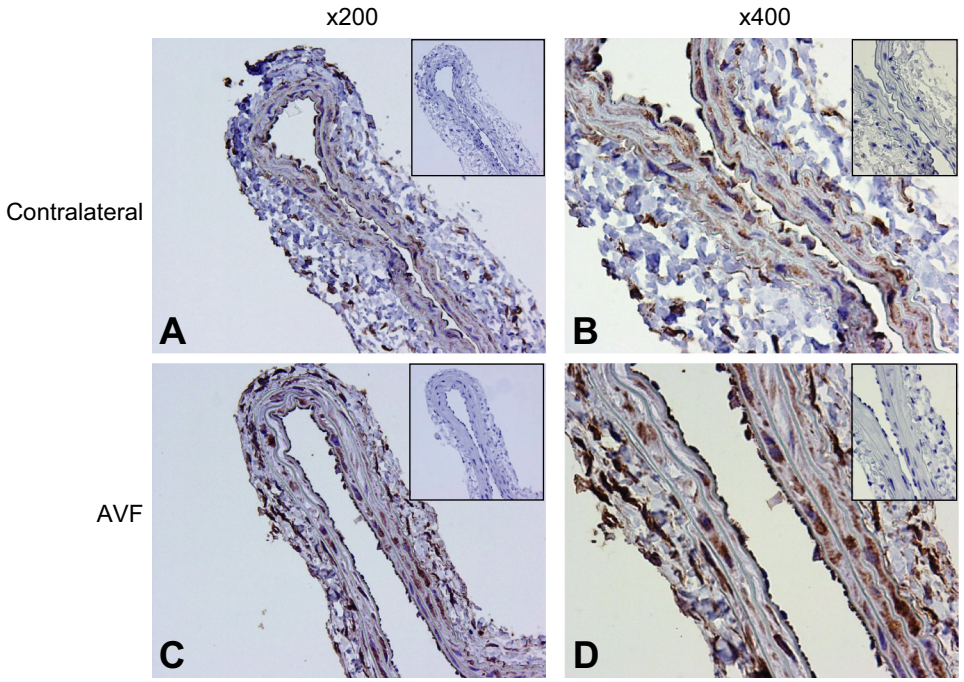

Fig. 1. Immunohistochemical (IHC) localization of heme oxygenase (HO)-2 expression in the arterial limb of the murine arteriovenous fistula (AVF) 2 wk after AVF creation. Low-power (*A* and *C*; ×200) and high-power (*B* and *D*: ×400) views of HO-2 protein expression in the arterial limb of AVF (*C* and *D*) and contralateral carotid artery (*A* and *B*) are shown. Each *inset* displays a nonimmune rabbit IgG incubation performed as negative control staining.

increase in AVF blood flow was completely absent in the setting of HO-2 deficiency in these studies undertaken at 4 wk (Fig. 4). Moreover, AVF failure, defined as the lack of discernible and measurable blood flow through the AVF, was markedly increased in the setting of HO-2 deficiency (Fig. 5).

Histological analyses were undertaken at the juxta-anastomotic region in the AVF for luminal narrowing as a consequence of neointimal hyperplasia, mural thrombus, and vessel wall thickening. Although there was an approximately twofold or greater increase in the percentages of AVFs in HO-$2^{-/-}$ mice compared with AVFs in HO-$2^{+/+}$ mice with occlusive luminal narrowing >75% (46 vs. 17%, AVF in HO-$2^{-/-}$ mice vs. AVF in. HO-$2^{+/+}$ mice) and luminal narrowing >50% (64 vs. 33%, AVF in HO-$2^{-/-}$ mice vs. AVF in HO-$2^{+/+}$ mice), these findings did not achieve statistical significance.

Our prior studies demonstrated that the exacerbatory effect of HO-1 deficiency in the AVF arose, in part, from exaggerated induction of matrix metalloproteinase (MMP)-9, a mitogenic, vasculopathic molecule (20). We thus examined expression of MMP-9 in the AVF. As shown in Fig. 6, HO-2 deficiency increased MMP-9 mRNA expression twofold in the AVF. However, expression of HO-1 in the AVF in HO-$2^{+/+}$ and

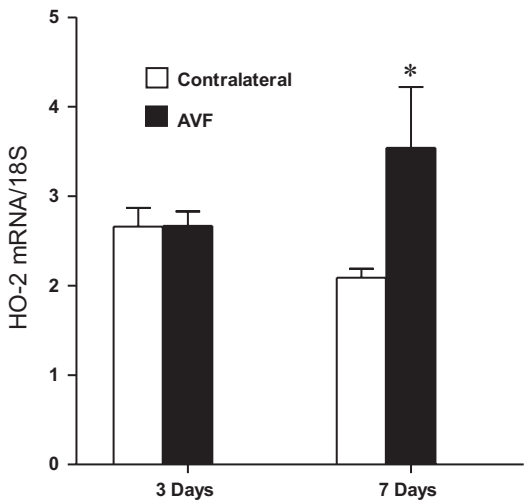

Fig. 2. Expression of HO-2 in the arterial limb of the AVF 3 days and 7 days after AVF creation in C57Bl6J mice. HO-2 mRNA expression in the arterial limb of the AVF and the contralateral carotid artery was determined by quantitative real-time RT-PCR 3 days ($n = 8$ and $n = 9$ in the AVF and contralateral groups, respectively) and 7 days ($n = 10$ and $n = 9$ in the AVF and contralateral groups, respectively) after AVF creation. Values are means ± SE. *$P < 0.05$ vs. contralateral group on that day.

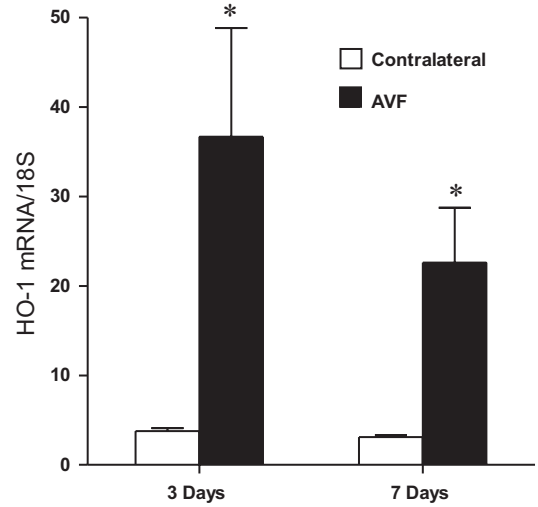

Fig. 3. Expression of HO-1 in the arterial limb of the AVF 3 days and 7 days after AVF creation in C57Bl6J mice. HO-1 mRNA expression in the arterial limb of the AVF and the contralateral carotid artery was determined by quantitative real-time RT-PCR 3 days ($n = 8$ and $n = 9$ in the AVF and contralateral groups, respectively) and 7 days ($n = 10$ and $n = 9$ in the AVF and contralateral groups, respectively) after AVF creation. Values are means ± SE. *$P < 0.05$ vs. contralateral group on that day.

Downloaded from journals.physiology.org/journal/ajprenal (065.021.193.086) on March 2, 2022.

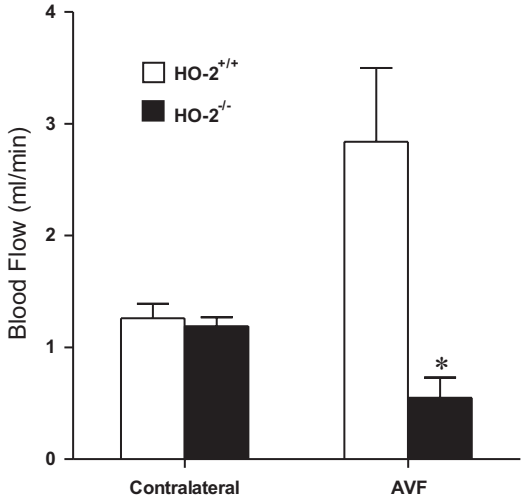

Fig. 4. Blood flow in the AVF in HO-$2^{+/+}$ and HO-$2^{-/-}$ mice 4 wk after AVF creation. Blood flow was measured in the arterial limb of the AVF and the contralateral artery in HO-$2^{+/+}$ and HO-$2^{-/-}$ mice with a perivascular flow probe ($n = 17$ and $n = 14$ in HO-$2^{+/+}$ and HO-$2^{-/-}$ groups, respectively). Values are means ± SE. *$P < 0.05$ vs. HO-$2^{+/+}$ AVF.

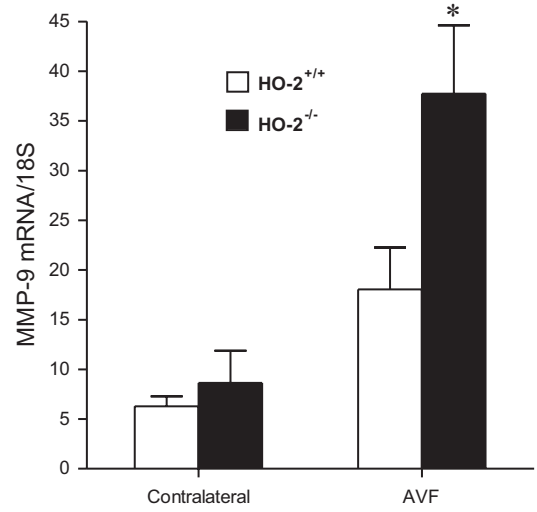

Fig. 6. Expression of matrix metalloproteinase (MMP)-9 in the arterial limb of the AVF in HO-$2^{+/+}$ and HO-$2^{-/-}$ mice. MMP-9 mRNA expression was determined by quantitative real-time RT-PCR in the arterial limb of the AVF and in the contralateral carotid artery in HO-$2^{+/+}$ and HO-$2^{-/-}$ mice 1 wk after AVF creation ($n = 6$ and $n = 5$ for HO-$2^{+/+}$ and HO-$2^{-/-}$ contralateral groups, respectively; $n = 12$ for each of the AVF groups). Values are means ± SE. *$P < 0.05$ vs. HO-$2^{+/+}$ AVF.

HO-$2^{-/-}$ mice was comparable (Fig. 7); thus neither the deterioration in AVF function nor the increased AVF expression of MMP-9, incurred by HO-2 deficiency, could be ascribed to blunted induction of HO-1. Furthermore, this increased induction of MMP-9 mRNA in the AVF in HO-2-deficient mice was not accompanied by increased expression of MMP-2 mRNA (Fig. 8), as was indeed the case in prior studies of the AVF in HO-$1^{-/-}$ mice.

We next questioned whether intrinsic abnormalities in vasorelaxation exist in the carotid artery in the setting of HO-2 deficiency, since such functional defects may contribute to impaired AVF function. We thus examined in vitro vasorelaxant responses of the carotid artery in HO-$2^{+/+}$ and HO-$2^{-/-}$ mice. However, neither endothelium-dependent nor endothelium-independent vasorelaxant responses were different in HO-$2^{+/+}$ and HO-$2^{-/-}$ mice (Figs. 9 and 10, respectively). These findings are consistent with measurements of acetylcholine-induced increments in carotid artery blood flow in vivo that were comparable in HO-$2^{+/+}$ and HO-$2^{-/-}$ mice (0.14 ± 0.02 and 0.11 ± 0.02 ml/min, $n = 6$ in each group, P = not significant).

AVFs are created in an uremic environment. We thus questioned whether AVF blood flow in the uremic milieu is impaired by concomitant deficiency of HO-2. Two weeks after subtotal nephrectomy was performed in HO-$2^{+/+}$ and HO-$2^{-/-}$ mice, an AVF was created by anastomosing the right carotid artery and the right jugular vein. Two weeks after the

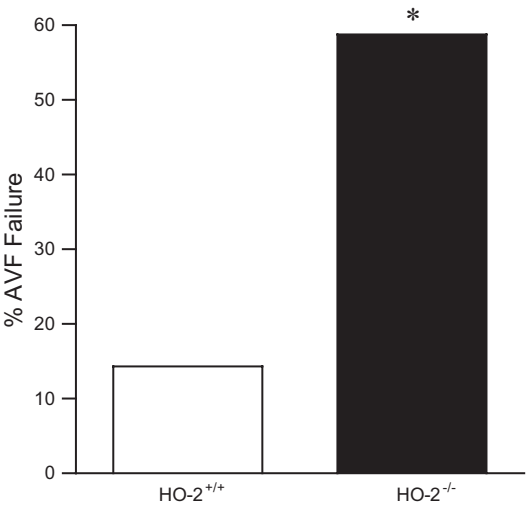

Fig. 5. AVF failure in HO-$2^{+/+}$ and HO-$2^{-/-}$ mice 4 wk after creation of the AVF. Percentages of failed AVFs in HO-$2^{+/+}$ and HO-$2^{-/-}$ mice, defined by visual assessment and absence of measured blood flow at this time point, are shown ($n = 17$ and $n = 14$ in HO-$2^{+/+}$ and HO-$2^{-/-}$ groups, respectively). *$P < 0.05$ vs. HO-$2^{+/+}$.

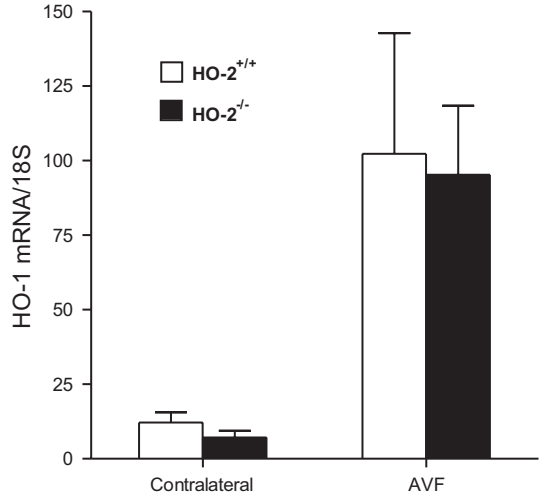

Fig. 7. Expression of HO-1 in the arterial limb of the AVF in HO-$2^{+/+}$ and HO-$2^{-/-}$ mice. HO-1 mRNA expression was determined by quantitative real-time RT-PCR in the arterial limb of the AVF and in the contralateral carotid artery in HO-$2^{+/+}$ and HO-$2^{-/-}$ mice 1 wk after AVF creation ($n = 6$ and $n = 5$ for HO-$2^{+/+}$ and HO-$2^{-/-}$ contralateral groups, respectively; $n = 12$ for each of the AVF groups). Values are means ± SE.

Downloaded from journals.physiology.org/journal/ajprenal (065.021.193.086) on March 2, 2022.

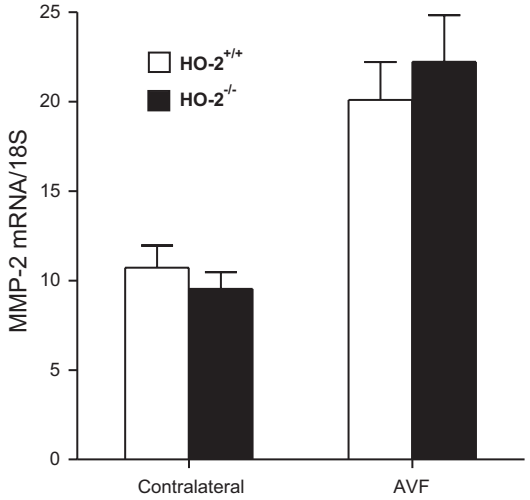

Fig. 8. Expression of MMP-2 in the arterial limb of the AVF in HO-$2^{+/+}$ and HO-$2^{-/-}$ mice. MMP-2 mRNA expression was determined by quantitative real-time RT-PCR in the arterial limb of the AVF and in the contralateral carotid artery in HO-$2^{+/+}$ and HO-$2^{-/-}$ mice 1 wk after AVF creation (n = 6 and n = 5 for HO-$2^{+/+}$ and HO-$2^{-/-}$ contralateral groups, respectively; n = 12 for each of the AVF groups). Values are means ± SE.

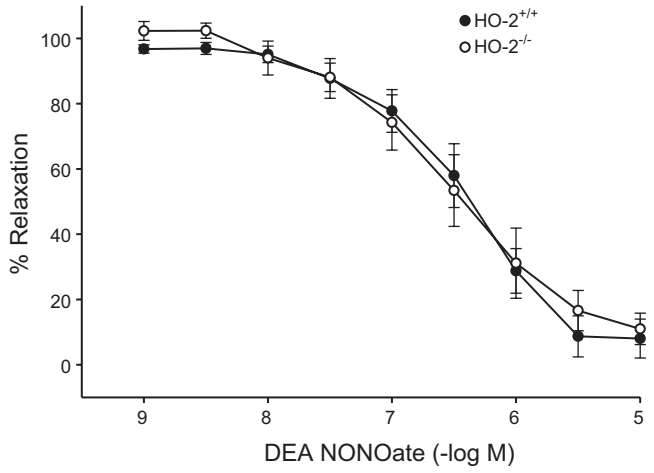

Fig. 10. Endothelium-independent relaxation in HO-$2^{+/+}$ and HO-$2^{-/-}$ mice. Endothelium-independent relaxation of the carotid artery is plotted in response to DEA NONOate in HO-$2^{+/+}$ and HO-$2^{-/-}$ mice (n = 7 in each group). Values are means ± SE. There were no significant differences in these responses in HO-$2^{+/+}$ and HO-$2^{-/-}$ mice.

creation of the AVF, AVF blood flow was determined. At this time point, there were no significant differences in body weight (29 ± 1 vs. 29 ± 1 g), hematocrit (41 ± 1 vs. 41 ± 1%), or BUN (56 ± 5 vs. 57 ± 4 mg/dl) in HO-$2^{+/+}$ and HO-$2^{-/-}$ mice subjected to the uremia followed by the AVF. AVF blood flow in these groups is shown in Fig. 11; as demonstrated, AVF blood flow, measured 2 wk after AVF creation in uremic mice, was reduced in the setting of HO-2 deficiency; deficiency of HO-2 did not significantly reduce blood flow in the intact, contralateral artery in the uremic milieu. It should be noted that these AVF blood flow studies were performed 2 wk after AVF creation, whereas studies summarized in Fig. 4 were performed after 4 wk; in this AVF model, decrease in blood flow and AVF closure start at ~3 wk.

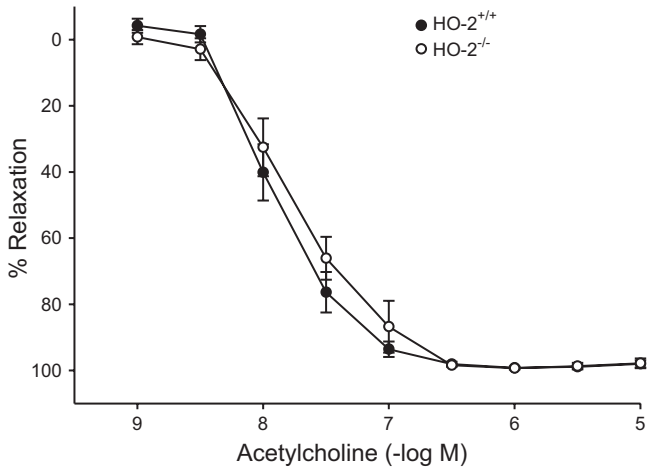

Fig. 9. Endothelium-dependent relaxation in HO-$2^{+/+}$ and HO-$2^{-/-}$ mice. Endothelium-dependent relaxation of the carotid artery is plotted in response to acetylcholine in HO-$2^{+/+}$ and HO-$2^{-/-}$ mice (n = 7 in each group). Values are means ± SE. There were no significant differences in these responses in the carotid artery in HO-$2^{+/+}$ and HO-$2^{-/-}$ mice.

DISCUSSION

The present studies demonstrate that the genetic absence of HO-2 substantially impairs the function of the murine AVF, and taken together with prior studies that specifically addressed the role of HO-1 in the AVF (20), they support the contribution of both the constitutive and inducible isoforms of HO in enabling functional adaptation following the creation of an AVF; additionally, these studies demonstrate that loss of either HO isoform is not redressed by the presence of the other in preserving the functionality of an AVF.

HO-2 protein is prominently expressed in the intact murine vasculature, and somewhat more so in the AVF, as shown in immunohistochemical analysis undertaken at 2 wk. In the preceding time frame, HO-2 mRNA expression in the AVF

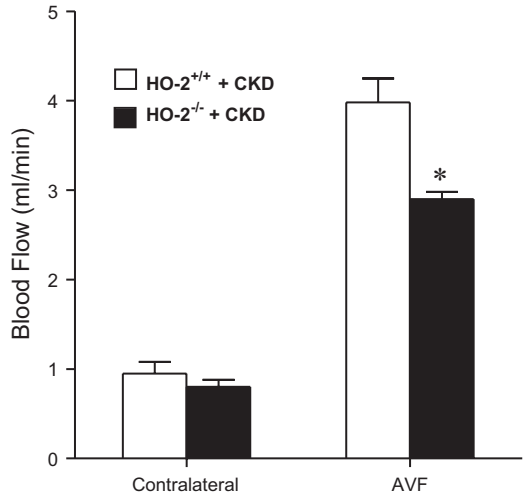

Fig. 11. Blood flow in the AVF in HO-$2^{+/+}$ and HO-$2^{-/-}$ mice with chronic kidney disease (CKD). Blood flow was measured in the arterial limb of the AVF and the contralateral carotid artery in HO-$2^{+/+}$ and HO-$2^{-/-}$ mice that were subjected to subtotal nephrectomy 2 wk before AVF creation (CKD) (n = 8 in each group). Measurements of AVF blood flow were undertaken at 2 wk after AVF creation. Values are means ± SE. *$P < 0.05$ vs. HO-$2^{+/+}$ AVF with CKD.

Downloaded from journals.physiology.org/journal/ajprenal (065.021.193.086) on March 2, 2022.

was unchanged at 3 days and modestly induced at 1 wk, thus differing sharply from the robust induction observed for HO-1 mRNA in the AVF in the same vascular segments and at the same time points. Certain distinct features of HO-2 and HO-1 merit consideration as regards their relative functional effects in the vasculature. First, because HO-2, unlike HO-1, is constitutively expressed and already in place in the vasculature, the vasorelaxant actions of HO-2 are tonically exerted at the time of AVF creation and not recruited thereafter (and thus delayed) as is the case for HO-1, which necessitates an obligatory period of induction. Second, HO activity from HO-2 is controlled and measured and not the robust, even fulminant, activity engendered by induction of HO-1; such marked induction of HO-1 and attendant HO activity may generate products of HO activity in such quantities that vasoprotective effects may not necessarily ensue. Third, the biological effects of the HO system may depend on not just HO activity but also signaling by the specific HO-1 and HO-2 proteins (23, 24, 28); notably, HO-1 and HO-2 represent distinct genes that generate specific proteins (1, 31). Fourth, an analogy with the isoforms of nitric oxide synthase (NOS) may be considered: although constitutive endothelial (eNOS) and inducible NOS (iNOS) have the same enzymic activities, their functional significance in physiological and pathophysiological states may substantially differ, and the behavior of one isoform cannot be used to predict the behavior of the other. The present studies demonstrate the importance of constitutive HO-2 expression in the adaptive responses that underlie enhanced blood flow following the creation of an AVF.

To determine whether deficiency of HO-2 was attended by an intrinsic abnormality in vascular behavior, we directly examined the vascular reactivity of the carotid artery. To our surprise, the absence of HO-2 in the carotid artery impaired neither endothelium-dependent nor endothelium-independent vasorelaxation of the carotid artery. Such similarity in carotid vascular reactivity in vitro in HO-$2^{+/+}$ and HO-$2^{-/-}$ mice was accompanied by similar increments in acetylcholine-induced carotid blood flow in vivo and comparable blood flow in the intact carotid artery (contralateral to the AVF) in HO-$2^{+/+}$ and HO-$2^{-/-}$ mice. Thus preexisting abnormalities either in vasorelaxant responses or in carotid blood flow cannot be implicated as contributory mechanisms in the failure of blood flow to increase when an AVF is created in the setting of HO-2 deficiency. However, unlike this seeming lack of a functional effect of deficiency of HO-2 in the intact, "unstressed" vasculature, such deficiency of HO-2 significantly impairs vascular behavior when the vasculature is subjected to hemodynamic stress as imposed by the creation of an AVF. Furthermore, HO-2 was also required in augmenting AVF blood flow when such hemodynamic stress was imposed in the presence of CKD, the latter representing the setting in which the AVF is created for use as a hemodialysis vascular access.

Our prior studies demonstrated that deficiency of HO-1 impairs the functionality of the AVF, an effect likely reflecting, in part, exaggerated expression of MMP-9. Substantial evidence indicates that MMP-9 exerts vasculopathic effects that include the marked stimulation of proliferation and migration of smooth muscle cells and proinflammatory effects (6, 9, 46); upregulation of MMP-9 is implicated in the promotion of neotimal hyperplasia in the injured vasculature and assorted vasculopathies that include dysfunction of hemodialysis vascular accesses (6, 7, 8, 9, 10, 20, 25, 29, 33, 46). We thus examined expression of MMP-9 and HO-1 in the AVF in HO-$2^{+/+}$ and HO-$2^{-/-}$ mice. We observed that the induction of MMP-9 in the AVF was exaggerated in the setting of HO-2 deficiency, whereas HO-1 was comparably induced in the AVF in HO-$2^{+/+}$ and HO-$2^{-/-}$ mice. This indicates that HO-2, as distinct from HO-1, may exert a suppressive effect on MMP-9 in the AVF. Also of note is that the observed augmented expression of MMP-9 in the AVF, induced by the deficiency of HO-2, was not accompanied by augmented induction of MMP-2, as was the case in prior studies in the AVF when MMP-9 expression was exaggerated by HO-1 deficiency. Interestingly, levels of MMP-9 are increased in uremia (35), and it is thus tempting to speculate that the impairment in AVF blood flow induced by HO-2 deficiency when the AVF is created in the uremic milieu may reflect further augmentation in MMP-9 levels.

Other cellular effects of HO-2, in addition to those involving suppression of MMP-9, may be relevant to the observed findings. HO-2, for example, is a survival factor in the endothelium as shown by the observations that HO-2 deficiency exacerbates apoptosis of endothelial cells incurred by either glutamate or TNF-α (3, 34), whereas increased amounts of HO-2 protein reduce the lethal effects of hypoxia in endothelial cells (18). Deficiency of HO-2 promotes the appearance of an activated phenotype in aortic endothelial cells (4), and following the wounding of the corneal epithelium, deficiency of HO-2 enhances inflammatory responses and impairs reparative responses (5, 17). Exacerbation of inflammatory responses induced by the deficiency of HO-2 may thus contribute to the decreased AVF flow and increased AVF failure observed in HO-2-deficient mice.

A relative merit of an approach based on HO-$2^{-/-}$ mice, compared with the use of chemical inhibitors of HO activity, is that such mutant mice enable the assessment of the specific involvement of the HO-2 isoform in pathophysiological states; however, relatively few studies to date have employed this approach in examining the role of HO-2 in vasorelaxant responses. Based on analyses in HO-$2^{-/-}$ mice, the conclusion has been reached that HO-2 contributes, in part, to acetylcholine-induced dilation of pial arterioles (38), whereas other studies have demonstrated that CO emanating from HO-2 may be vasoconstrictive in pial arterioles and that hypoxia induces cerebral vasodilation by suppressing generation of CO by HO-2 (30). Neither hypoxia-induced pulmonary hypertension nor reduction in renal blood flow incurred by angiotensin II or nitro-L-arginine methyl ester (L-NAME) is altered by the genetic deficiency of HO-2 (39, 43). A mild increase in blood pressure (not observed in the present studies or in prior studies) has been described in HO-$2^{-/-}$ mice, along with an impaired vasorelaxant response in aortic rings (42). The present studies demonstrate that chronic augmentation in blood flow as occurs in an AVF is fundamentally dependent on HO-2, but they do not reveal an intrinsic impairment in acute vasorelaxation of the carotid artery either in vitro or in vivo. It would be of interest whether other states attended by chronic augmentation in systemic or regional blood flow require HO-2 for such a response, including states characterized by increased renal blood flow such as diabetes mellitus, following uninephrectomy, high dietary protein intake, and pregnancy.

Downloaded from journals.physiology.org/journal/ajprenal (065.021.193.086) on March 2, 2022.

In summary, to the best of our knowledge, the present studies are the first to examine and demonstrate the functional significance of vascular expression of the constitutive HO isoform HO-2 in the AVF: although without a discernible functional effect in the unstressed vasculature, HO-2 is required for maintaining augmented blood flow in the vasculature subjected to the chronic hemodynamic stress imposed by an AVF, either in the setting of intact renal function or in the uremic milieu. On the basis of our findings, we speculate that variability in constitutive expression of HO-2 may be considered as a possible contributor to the unacceptably high failure rates for maturation of AVFs when employed as hemodialysis vascular accesses and that HO-2 may be the target of novel therapeutic approaches seeking to promote the maturation and longevity of hemodialysis AVFs.

ACKNOWLEDGMENTS

We gratefully acknowledge the secretarial expertise of Brittney Lewis in the preparation of the manuscript.

GRANTS

These studies were supported by National Institute of Diabetes and Digestive and Kidney Diseases Grants DK47060 and DK70124.

DISCLOSURES

No conflicts of interest, financial or otherwise, are declared by the authors.

AUTHOR CONTRIBUTIONS

K.A.N., L.K., A.J.C., and Z.S.K., conception and design of research; L.K., A.J.C., and Z.S.K. performed experiments; K.A.N., L.K., J.P.G., G.F., A.J.C., and Z.S.K. analyzed data; K.A.N., L.K., J.P.G., G.F., A.J.C., and Z.S.K. interpreted results of experiments; A.J.C. and Z.S.K. prepared figures; K.A.N., L.K., A.J.C. drafted manuscript; K.A.N., L.K., A.J.C., and Z.S.K. edited and revised manuscript; K.A.N., L.K., J.P.G., G.F., A.J.C., and Z.S.K. approved final version of manuscript.

REFERENCES

1. **Agarwal A, Nick HS.** Renal response to tissue injury: lessons from heme oxygenase-1 gene ablation and expression. *J Am Soc Nephrol* 11: 965–973, 2000.
2. **Allon M.** Current management of vascular access. *Clin J Am Soc Nephrol* 2: 786–800, 2007.
3. **Basuroy S, Bhattacharya S, Tcheranova D, Qu Y, Regan RF, Leffler CW, Parfenova H.** HO-2 provides endogenous protection against oxidative stress and apoptosis caused by TNF-alpha in cerebral vascular endothelial cells. *Am J Physiol Cell Physiol* 291: C897–C908, 2006.
4. **Bellner L, Martinelli L, Halilovic A, Patil K, Puri N, Dunn MW, Regan RF, Schwartzman ML.** Heme oxygenase-2 deletion causes endothelial cell activation marked by oxidative stress, inflammation, and angiogenesis. *J Pharmacol Exp Ther* 331: 925–932, 2009.
5. **Bellner L, Patil KA, Castellano K, Halilovic A, Dunn MW, Schwartzman ML.** Targeted suppression of HO-2 gene expression impairs the innate anti-inflammatory and repair responses of the cornea to injury. *Mol Vis* 17: 1144–1152, 2011.
6. **Bendeck MP, Conte M, Zhang M, Nili N, Strauss BH, Farwell SM.** Doxycycline modulates smooth muscle cell growth, migration, and matrix remodeling after arterial injury. *Am J Pathol* 160: 1089–1095, 2002.
7. **Chan CY, Chen YS, Ma MC, Chen CF.** Remodeling of experimental arteriovenous fistula with increased matrix metalloproteinase expression in rats. *J Vasc Surg* 45: 804–811, 2007.
8. **Chang CJ, Ko YS, Ko PJ, Hsu LA, Chen CF, Yang CW, Hsu TS, Pang JH.** Thrombosed arteriovenous fistula for hemodialysis access is characterized by a marked inflammatory activity. *Kidney Int* 68: 1312–1319, 2005.
9. **Cho A, Reidy MA.** Matrix metalloproteinase-9 is necessary for the regulation of smooth muscle cell replication and migration after arterial injury. *Circ Res* 91: 845–851, 2002.
10. **Croatt AJ, Grande JP, Hernandez MC, Ackerman AW, Katusic ZS, Nath KA.** Characterization of a model of an arteriovenous fistula in the rat: the effect of L-NAME. *Am J Pathol* 176: 2530–2541, 2010.
11. **d'Uscio LV, Smith LA, Katusic ZS.** Hypercholesterolemia impairs endothelium-dependent relaxations in common carotid arteries of apolipoprotein e-deficient mice. *Stroke* 32: 2658–2664, 2001.
12. **d'Uscio LV, Smith LA, Santhanam AV, Richardson D, Nath KA, Katusic ZS.** Essential role of endothelial nitric oxide synthase in vascular effects of erythropoietin. *Hypertension* 49: 1142–1148, 2007.
13. **Farrugia G, Lei S, Lin X, Miller SM, Nath KA, Ferris CD, Levitt M, Szurszewski JH.** A major role for carbon monoxide as an endogenous hyperpolarizing factor in the gastrointestinal tract. *Proc Natl Acad Sci USA* 100: 8567–8570, 2003.
14. **Gagnon RF, Duguid WP.** A reproducible model for chronic renal failure in the mouse. *Urol Res* 11: 11–14, 1983.
15. **Gagnon RF, Gallimore B.** Characterization of a mouse model of chronic uremia. *Urol Res* 16: 119–126, 1988.
16. **Hakim RM, Himmelfarb J.** Hemodialysis access failure: a call to action–revisited. *Kidney Int* 76: 1040–1048, 2009.
17. **Halilovic A, Patil KA, Bellner L, Marrazzo G, Castellano K, Cullaro G, Dunn MW, Schwartzman ML.** Knockdown of heme oxygenase-2 impairs corneal epithelial cell wound healing. *J Cell Physiol* 226: 1732–1740, 2011.
18. **He JZ, Ho JJ, Gingerich S, Courtman DW, Marsden PA, Ward ME.** Enhanced translation of heme oxygenase-2 preserves human endothelial cell viability during hypoxia. *J Biol Chem* 285: 9452–9461, 2010.
19. **Juncos JP, Grande JP, Kang L, Ackerman AW, Croatt AJ, Katusic ZS, Nath KA.** MCP-1 contributes to arteriovenous fistula failure. *J Am Soc Nephrol* 22: 43–48, 2011.
20. **Juncos JP, Tracz MJ, Croatt AJ, Grande JP, Ackerman AW, Katusic ZS, Nath KA.** Genetic deficiency of heme oxygenase-1 impairs functionality and form of an arteriovenous fistula in the mouse. *Kidney Int* 74: 47–51, 2008.
21. **Kang L, Yamada S, Hernandez MC, Croatt AJ, Grande JP, Juncos JP, Vercellotti GM, Hebbel RP, Katusic ZS, Terzic A, Nath KA.** Regional and systemic hemodynamic responses following the creation of a murine arteriovenous fistula. *Am J Physiol Renal Physiol* 301: F845–F851, 2011.
22. **Kanwar YS.** Functional duality of progenitor cells influxing into arteriovenous fistula during its neoangiogenesis. *Am J Physiol Renal Physiol* 293: F468–F469, 2007.
23. **Kim YS, Dore S.** Catalytically inactive heme oxygenase-2 mutant is cytoprotective. *Free Radic Biol Med* 39: 558–564, 2005.
24. **Kim YS, Zhuang H, Koehler RC, Dore S.** Distinct protective mechanisms of HO-1 and HO-2 against hydroperoxide-induced cytotoxicity. *Free Radic Biol Med* 38: 85–92, 2005.
25. **Lambert V, Munaut C, Jost M, Noel A, Werb Z, Foidart JM, Rakic JM.** Matrix metalloproteinase-9 contributes to choroidal neovascularization. *Am J Pathol* 161: 1247–1253, 2002.
26. **Lee T, Roy-Chaudhury P.** Advances and new frontiers in the pathophysiology of venous neointimal hyperplasia and dialysis access stenosis. *Adv Chronic Kidney Dis* 16: 329–338, 2009.
27. **Lee T, Wadehra D.** Genetic causation of neointimal hyperplasia in hemodialysis vascular access dysfunction. *Semin Dial* 25: 65–73, 2012.
28. **Lin Q, Weis S, Yang G, Weng YH, Helston R, Rish K, Smith A, Bordner J, Polte T, Gaunitz F, Dennery PA.** Heme oxygenase-1 protein localizes to the nucleus and activates transcription factors important in oxidative stress. *J Biol Chem* 282: 20621–20633, 2007.
29. **Misra S, Fu AA, Rajan DK, Juncos LA, McKusick MA, Bjarnason H, Mukhopadhyay D.** Expression of hypoxia inducible factor-1 alpha, macrophage migration inhibition factor, matrix metalloproteinase-2 and -9, and their inhibitors in hemodialysis grafts and arteriovenous fistulas. *J Vasc Interv Radiol* 19: 252–259, 2008.
30. **Morikawa T, Kajimura M, Nakamura T, Hishiki T, Nakanishi T, Yukutake Y, Nagahata Y, Ishikawa M, Hattori K, Takenouchi T, Takahashi T, Ishii I, Matsubara K, Kabe Y, Uchiyama S, Nagata E, Gadalla MM, Snyder SH, Suematsu M.** Hypoxic regulation of the cerebral microcirculation is mediated by a carbon monoxide-sensitive hydrogen sulfide pathway. *Proc Natl Acad Sci USA* 109: 1293–1298, 2012.
31. **Nath KA.** Heme oxygenase-1: a provenance for cytoprotective pathways in the kidney and other tissues. *Kidney Int* 70: 432–443, 2006.
32. **Nath KA, Grande JP, Farrugia G, Croatt AJ, Belcher JD, Hebbel RP, Vercellotti GM, Katusic ZS.** Age sensitizes the kidney to heme protein-

Downloaded from journals.physiology.org/journal/ajprenal (065.021.193.086) on March 2, 2022.

induced acute kidney injury. *Am J Physiol Renal Physiol* 304: F317–F325, 2013.
33. **Newby AC.** Do metalloproteinases destabilize vulnerable atherosclerotic plaques? *Curr Opin Lipidol* 17: 556–561, 2006.
34. **Parfenova H, Basuroy S, Bhattacharya S, Tcheranova D, Qu Y, Regan RF, Leffler CW.** Glutamate induces oxidative stress and apoptosis in cerebral vascular endothelial cells: contributions of HO-1 and HO-2 to cytoprotection. *Am J Physiol Cell Physiol* 290: C1399–C1410, 2006.
35. **Pawlak K, Mysliwiec M, Pawlak D.** Peripheral blood level alterations of MMP-2 and MMP-9 in patients with chronic kidney disease on conservative treatment and on hemodialysis. *Clin Biochem* 44: 838–843, 2011.
36. **Pittock ST, Norby SM, Grande JP, Croatt AJ, Bren GD, Badley AD, Caplice NM, Griffin MD, Nath KA.** MCP-1 is up-regulated in unstressed and stressed HO-1 knockout mice: pathophysiologic correlates. *Kidney Int* 68: 611–622, 2005.
37. **Poss KD, Thomas MJ, Ebralidze AK, O'Dell TJ, Tonegawa S.** Hippocampal long-term potentiation is normal in heme oxygenase-2 mutant mice. *Neuron* 15: 867–873, 1995.
38. **Qin X, Kwansa H, Bucci E, Dore S, Boehning D, Shugar D, Koehler RC.** Role of heme oxygenase-2 in pial arteriolar response to acetylcholine in mice with and without transfusion of cell-free hemoglobin polymers. *Am J Physiol Regul Integr Comp Physiol* 295: R498–R504, 2008.
39. **Roth M, Rupp M, Hofmann S, Mittal M, Fuchs B, Sommer N, Parajuli N, Quanz K, Schubert D, Dony E, Schermuly RT, Ghofrani HA, Sausbier U, Rutschmann K, Wilhelm S, Seeger W, Ruth P, Grimminger F, Sausbier M, Weissmann N.** Heme oxygenase-2 and large-conductance Ca^{2+}-activated K^+ channels: lung vascular effects of hypoxia. *Am J Respir Crit Care Med* 180: 353–364, 2009.
40. **Roy-Chaudhury P, Lee TC.** Vascular stenosis: biology and interventions. *Curr Opin Nephrol Hypertens* 16: 516–522, 2007.
41. **Schinstock CA, Albright RC, Williams AW, Dillon JJ, Bergstralh EJ, Jenson BM, McCarthy JT, Nath KA.** Outcomes of arteriovenous fistula creation after the Fistula First Initiative. *Clin J Am Soc Nephrol* 6: 1996–2002, 2011.
42. **Sodhi K, Inoue K, Gotlinger KH, Canestraro M, Vanella L, Kim DH, Manthati VL, Koduru SR, Falck JR, Schwartzman ML, Abraham NG.** Epoxyeicosatrienoic acid agonist rescues the metabolic syndrome phenotype of HO-2-null mice. *J Pharmacol Exp Ther* 331: 906–916, 2009.
43. **Stec DE, Vera T, Storm MV, McLemore GR Jr, Ryan MJ.** Blood pressure and renal blow flow responses in heme oxygenase-2 knockout mice. *Am J Physiol Regul Integr Comp Physiol* 297: R1822–R1828, 2009.
44. **Tsapenko MV, d'Uscio LV, Grande JP, Croatt AJ, Hernandez MC, Ackerman AW, Katusic ZS, Nath KA.** Increased production of superoxide anion contributes to dysfunction of the arteriovenous fistula. *Am J Physiol Renal Physiol* 303: F1601–F1607, 2012.
45. **Zarjou A, Agarwal A.** Superoxide in AVF dysfunction: a new target for intervention. *Am J Physiol Renal Physiol* 303: F1599–F1600, 2012.
46. **Zempo N, Kenagy RD, Au YP, Bendeck M, Clowes MM, Reidy MA, Clowes AW.** Matrix metalloproteinases of vascular wall cells are increased in balloon-injured rat carotid artery. *J Vasc Surg* 20: 209–217, 1994.

Downloaded from journals.physiology.org/journal/ajprenal (065.021.193.086) on March 2, 2022.